ACS OMEGA

http://pubs.acs.org/journal/acsodf

Article

Synthesis, Catalytic GPx-like Activity, and SET Reactions of Conformationally Constrained 2,7-Dialkoxy-Substituted Naphthalene-1,8-*peri*-diselenides

Adrian I. Doig, Tyler A. Tuck, Brandon LeBlanc, and Thomas G. Back*

Cite This: *ACS Omega* 2022, 7, 27312−27323

Read Online

ACCESS | Metrics & More | Article Recommendations | Supporting Information

ABSTRACT: Several 2,7-dialkoxy-substituted naphthalene-1,8-*peri*-diselenides were prepared and tested for catalytic antioxidant activity in an NMR-based assay employing the reduction of hydrogen peroxide with stoichiometric amounts of benzyl thiol. Acidic conditions enhanced their catalytic activity, whereas basic conditions suppressed it. The highest activity was observed with a 2,7-bis(triethyleneglycol) derivative. These compounds serve as mimetics of the antioxidant selenoenzyme glutathione peroxidase. Studies based on NMR peak-broadening effects and EPR spectroscopy indicated that a thiol-dependent SET reaction occurs under the conditions of the assay, which can be reversed by the addition of triethylamine. In contrast, peak broadening induced by proton-catalyzed electron transfer during the treatment of naphthalene-1,8-*peri*-diselenides with trifluoroacetic acid can be suppressed by the addition of excess thiol. These observations provide new insights into the redox mechanisms of these processes.

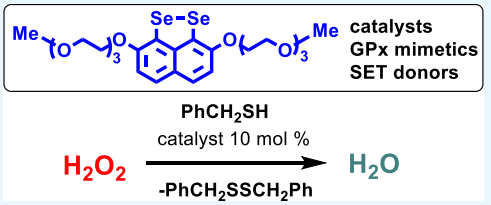

INTRODUCTION

Naphthalene *peri*-diselenide **1a** was first reported by Meinwald and Wudl *et al.*[1] by the lithiation and selenation of 1,8-dibromonaphthalene. This and related compounds have proven to be of interest as electron donors in charge transfer complexes and organic conductors.[2] Woollins *et al.* reported the solid-state ^{77}Se NMR spectrum[3] and X-ray crystal structure[4] of **1a**, as well as complexes of **1a** and its derivatives with various metals and metalloids.[5] Diselenide **1a** and its diselenol analogue also effect the deiodination of thyroxine, as demonstrated by Manna, Mugesh and Mondal,[6] while Grainger *et al.* employed **1a** and its congeners as mimetics of [FeFe]-hydrogenase.[7]

As part of our ongoing studies[8] of organoselenium compounds that serve as mimetics of the selenoenzyme glutathione peroxidase (GPx),[9] we considered that **1a** and its analogues might be effective for this purpose. GPx protects cells from oxidative stress caused by hydrogen peroxide and other reactive oxygen species (ROS) that are formed during aerobic metabolism by catalyzing the reduction of ROS with the tripeptide thiol glutathione.[10] Oxidative stress is in turn implicated in numerous diseases and degenerative conditions,[11] examples of which include reperfusion injury in heart attack and stroke patients,[12] as well as hearing loss,[13] for which the selenium compound ebselen has been tested in clinical trials. Ebselen is also in clinical trials as a lithium surrogate in the treatment of bipolar disorder.[14] In acute cases, where ROS levels are particularly elevated, GPx is overwhelmed, and administration of a supplementary antioxidant is desirable to suppress excessive oxidative stress.

Typically, acyclic diaryl diselenides have C−Se−Se−C dihedral angles that are close to orthogonal, presumably to minimize destabilizing selenium lone pair interactions. For example, the dihedral angle in diphenyl diselenide was determined to be 82.0° by X-ray crystallography.[15] However, several years ago we found that the highly sterically hindered diselenide **2** (Figure 1) displayed a dihedral angle of 112.1°, along with a bathochromic shift in its UV−visible spectrum compared to less hindered aliphatic diselenides.[16] This indicated that the conformational constraint imposed by the bulky *t*-butyl substituents forced an increase in the dihedral angle and simultaneously raised the energy level of the HOMO while decreasing the HOMO−LUMO gap in **2**. Since selenium

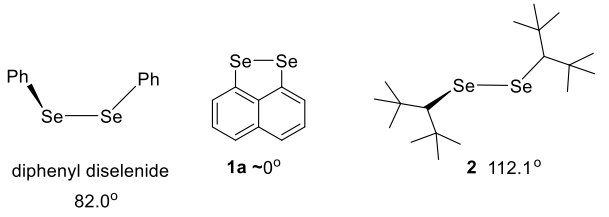

Figure 1. C−Se−Se−C dihedral angles of diselenides.

Received: April 12, 2022
Accepted: June 30, 2022
Published: July 28, 2022

Scheme 1. Synthesis of Naphthalene *peri*-Diselenides

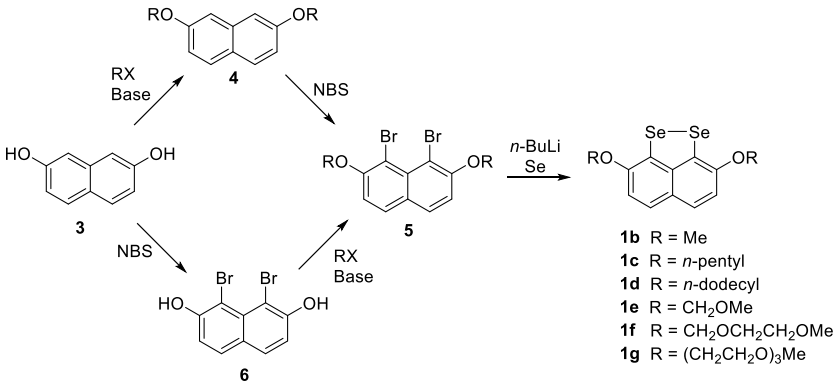

oxidation is generally the rate-determining step in the catalytic cycle of various GPx mimetics,[8a,17] this observation suggested that the catalytic activity of other diselenides might be further enhanced by constraining their dihedral angles from the usual nearly orthogonal geometry to a coplanar one, thus again raising their HOMO energies and lowering their oxidation potentials. The rigid naphthalene diselenide **1a**, where the C−Se−Se−C dihedral angle is essentially 0° (Figure 1), was chosen to test this possibility, as reported in our preliminary communication.[17] Thus, **1a** displayed catalytic activity ca. 13 times greater than that of diphenyl diselenide, while the 2,7-dimethoxy derivative **1b** revealed a further increase in activity to 17.4 times that of the diphenyl derivative, consistent with mesomeric stabilization of positive charge during the rate-determining selenium oxidation step. As a result, it was desirable to retain oxygen substituents at the 2- and 7-positions in the investigation of new compounds.

It is also recognized that intramolecular coordination can have profound effects on the reactivity of selenium compounds.[18,19] Since the angle strain associated with the four-centered O−Se interaction in **1b** impedes intramolecular coordination, it was of interest to investigate less studied structures where six- or seven-centered coordination might be possible. Moreover, the installation of longer alkoxy chains on the naphthalene moiety, along with more highly oxygenated analogues, would also provide a range of compounds with varying lipophilic and hydrophilic properties, for eventual optimization of bioavailability.

We had previously discovered that naphthalene *peri*-diselenides **1a−1c**, as well as their sulfur and tellurium analogues, undergo a facile proton-catalyzed electron transfer (PCET) reaction that could be suppressed under basic conditions, as evidenced by NMR and EPR experiments.[20] However, the effect of PCET or related processes on the catalytic GPx-like activity of naphthalene *peri*-diselenides was unknown. We now report the preparation of several additional 2,7-disubstituted analogues that contain either long-chain alkoxy substituents, or more highly oxygenated ones, and the in vitro assessment of their catalytic activities, as well as new insights into the mechanism of such processes.

RESULTS AND DISCUSSION

Compounds **1b**[17] and **1c**[20] were obtained by variations of the original method of Meinwald and Wudl,[1] along with new analogues **1d−1g**. In general, 2,7-dihydroxynaphthalene (**3**) was *O*-alkylated to afford **4** and brominated selectively at the 1,8-positions with *N*-bromosuccinimide (NBS), providing **5**. Metalation and selenation, followed by aerial oxidation, then afforded the desired products **1b−1g**. Alternatively, **3** was first brominated and then alkylated to afford **5** *via* **6**. These processes are summarized in Scheme 1.

With diselenides **1b−1g** in hand, we proceeded to measure their catalytic properties in promoting the reduction of hydrogen peroxide with benzyl thiol as the stoichiometric reductant. In our previous investigations of compounds **1a** and **1b**, an HPLC-based assay was successfully employed. However, the widely differing solubilities of the present range of diselenides in various available mobile phases precluded their direct comparison by HPLC analysis. Consequently, an NMR-based assay was developed, where each of **1b−1g** could be run under the same conditions. Thus, a mixture of benzyl thiol, dimethyl terephthalate (DMT, internal standard), and 10 mol % of the catalyst (relative to benzyl thiol) was stirred in $CDCl_3$-CD_3OD (95:5) at 18 °C. A small excess of 50% H_2O_2 was added, and the mixture was periodically analyzed by comparison of the NMR integration of the methylene singlet of dibenzyl disulfide at 3.57 ppm with the aryl signal of the internal standard at 8.06 ppm.[21] A typical NMR assay with diselenide **1b** as the catalyst is shown in Figure 2, indicating the increase in dibenzyl disulfide concentration with time. Each diselenide was run at least three times, and the averaged plots of % yield of dibenzyl disulfide versus time are provided in Figure 3. The linear

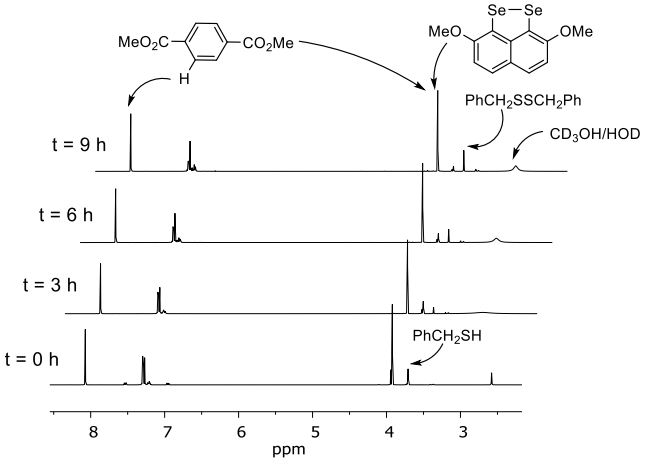

Figure 2. ^{1}H NMR assay of diselenide catalyst **1b** in the oxidation of benzyl thiol with hydrogen peroxide. The ^{1}H NMR spectra were recorded at 400 MHz in $CDCl_3$-CD_3OD (95:5).

https://doi.org/10.1021/acsomega.2c02286
ACS Omega 2022, 7, 27312−27323

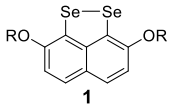

1

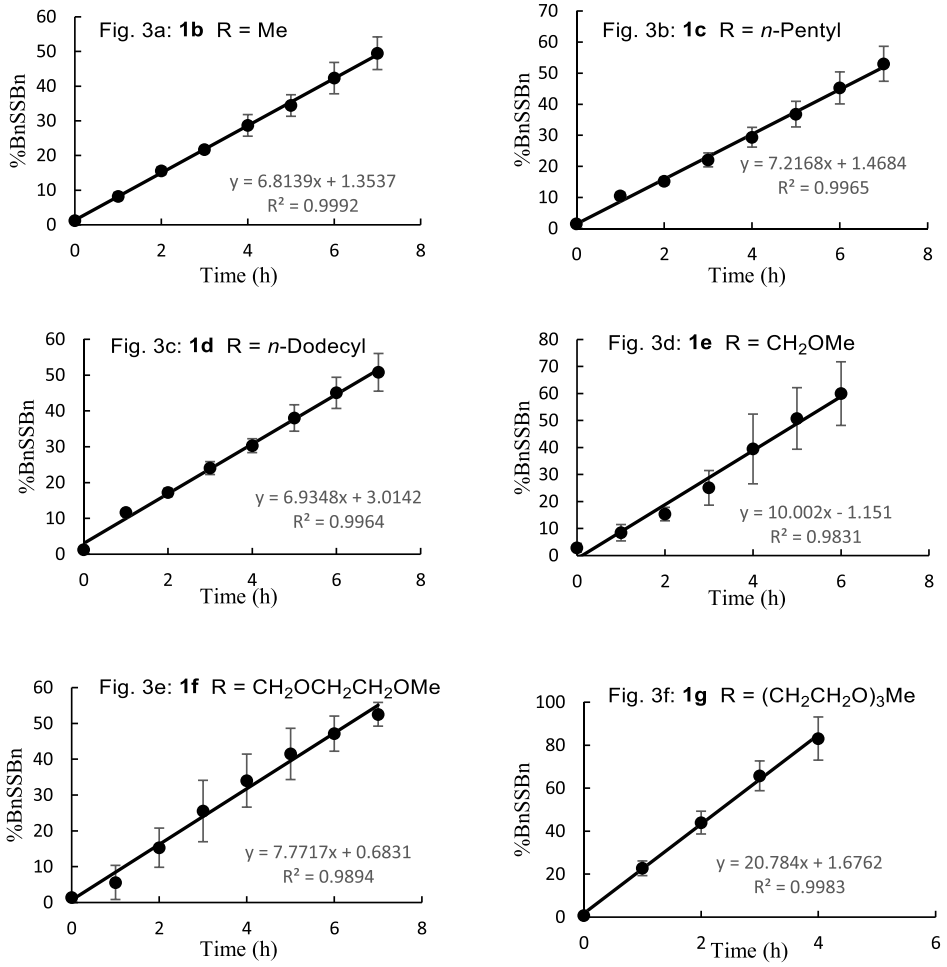

Figure 3. (a–f) Kinetic plots for assays of diselenide catalysts: (a) **1b**, (b) **1c**, (c) **1d**, (d) **1e**, (e) **1f**, (f) **1g**. Reactions were performed at 18 °C in $CDCl_3$–CD_3OD (95:5). Initial concentrations were as follows: benzyl thiol, 0.031 M; H_2O_2, 0.035 M; catalyst, 0.0031 M; and DMT, 0.0155 M. The formation of dibenzyl disulfide was monitored by ^1H NMR spectroscopy *via* integration of the disulfide methylene signal at 3.57 ppm *vs* the aromatic signal of DMT at 8.06 ppm. The plots are averages of either three or four runs.

nature of these plots is consistent with zero-order kinetics of a catalytic system. The time required for 50% completion of the oxidation of the thiol to its corresponding disulfide ($t_{1/2}$) also provides a convenient parameter for comparing the catalytic activities of various types of GPx mimetics.[8a,22] These values are provided for **1b**–**1g** in Table 1. Diphenyl diselenide and the unsubstituted naphthalene *peri*-diselenide **1a** are included for comparison.

These results indicate that the *n*-pentyloxy and *n*-dodecyloxy substituents of **1c** and **1d**, respectively, produced similar catalytic effects to that of the methoxy derivative **1b** (compare entries 7 and 8 with entry 3 in Table 1). This was expected because all three diselenides are subject to comparable mesomeric effects from electron-donating alkoxy groups but lack an additional nucleophilic center for coordination with selenium during the oxidation step. On the other hand, the methoxymethyl analogue **1e**, where a second oxygen is able to coordinate with selenium *via* a six-membered cyclic interaction, showed a modest improvement in activity [$t_{1/2}$ = 5.1 h for **1e** *vs* 7.1 h for **1b** (entries 9 and 3, respectively, in Table 1)], while such an enhancement was less evident in the (methoxyethoxy)methoxy analogue **1f** ($t_{1/2}$ = 6.5 h; entry 10, Table 1).[23] In contrast, the triethylene glycol derivative **1g** revealed a more pronounced effect, affording a significantly faster rate ($t_{1/2}$ = 2.3 h; entry 11, Table 1) than any of the other diselenides shown in Table 1.

The mechanism for the catalytic activity of **1a** and **1b** was reported in our preliminary communication[17] and is shown in more detail in Scheme 2. The diselenides were slowly oxidized by hydrogen peroxide to the isolable selenolseleninates **8**, presumably formed from the hydroxyselenonium intermediates **7**, followed by rapid reduction back to the parent diselenides by benzyl thiol *via* **9** and/or **10**. It is possible that the modest to significant rate enhancements observed in **1e**–**1g** are due to coordination effects, as shown by structure **11** (Figure 4), resulting in a further increase in the reactivity of the selenium atoms toward rate-determining oxidation. However, it is not entirely clear why **1g**, where such coordination would require a

https://doi.org/10.1021/acsomega.2c02286
ACS Omega 2022, 7, 27312–27323

Table 1. Catalytic Activities of Diselenides 1a−1g[a]

entry	diselenide	additive[b]	$t_{1/2}$ (h)[c]
1	PhSeSePh	nil	(129)
2	**1a**	nil	(9.7)
3	**1b**	nil	7.1 (7.4)
4	**1b**	1 mol % TFA	4.2
5	**1b**	10 mol % TFA	3.0
6	**1b**	100 mol % Py-d_5	13.4
7	**1c**	nil	6.7
8	**1d**	nil	6.8
9	**1e**	nil	5.1
10	**1f**	nil	6.5
11	**1g**	nil	2.3

[a]Reactions were performed at 18 °C in $CDCl_3$−CD_3OD (95:5). Initial concentrations were as follows: benzyl thiol, 0.031 M; H_2O_2, 0.035 M; catalyst, 0.0031 M; and DMT, 0.0155 M. [b]TFA is trifluoroacetic acid, and Py-d_5 is deuterated pyridine. [c]The values of $t_{1/2}$ (time taken for 50% completion of the oxidation of the thiol to its disulfide) are averages of either three or four runs. The values in parentheses were taken from ref 17 and were obtained under slightly different conditions *via* an HPLC-based assay.

Scheme 2. Catalytic Cycle for the Reduction of Hydrogen Peroxide with Naphthalene *peri*-Diselenides and Benzyl Thiol

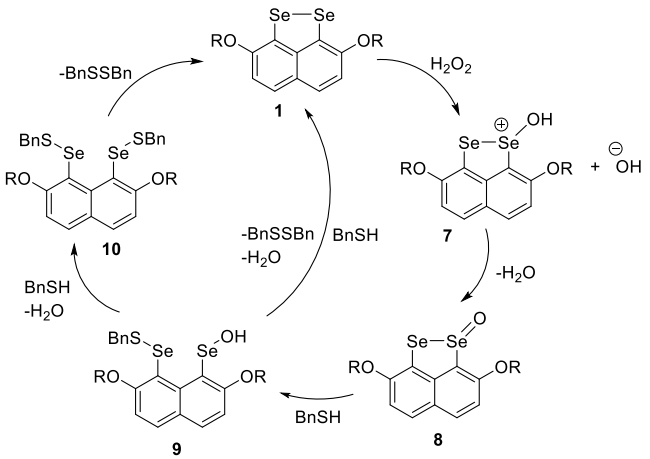

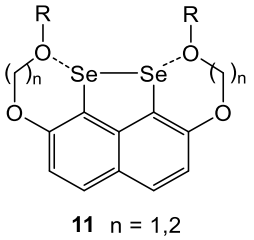

Figure 4. Possible O···Se coordination in naphthalene *peri*-diselenides **1e**−**1g**.

seven-membered or larger ring, produced a faster reaction than **1e** or **1f**, where enhanced coordination *via* a six-centered structure would be expected. A possible explanation is that the anomeric effect in acetals **1e** and **1f** (*i.e.*, structure **11** where n = 1 in Figure 4) decreases the magnitude of mesomeric electron donation from the alkoxy oxygen atom to the naphthalene diselenide moiety. Since electron donation increases the rate of the rate-determining oxidation of the diselenide moiety, the anomeric effect in **1e** and **1f** is expected to decrease their reaction rates relative to that of **1g** (*i.e.*, structure **11** where n = 2), where such anomeric deactivation is not possible.[24] However, the alkoxy derivatives **1b**−**1d**, where the anomeric effect is similarly precluded, also show lower reactivity than **1g**. In this case, the decreased reactivity may be attributed to the lack of a second oxygen atom capable of coordinating with selenium. Thus, the relative reaction rates of the diselenides, as shown in Table 1, are dependent upon a balance of mesomeric, coordination, and, in some examples, anomeric effects.

It was also of interest to determine whether the previously discovered PCET reaction of naphthalene *peri*-chalcogenides[20] (*e.g.*, as shown for **1b** in Scheme 3) played a role in the

Scheme 3. PCET Reaction of Naphthalene *peri*-Diselenide 1b

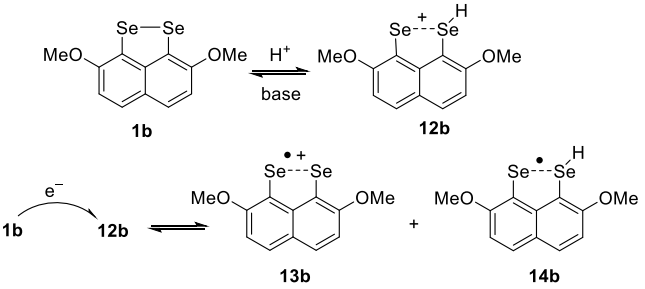

catalytic activity of compounds **1b**−**1g**. This phenomenon was first identified when various naphthalene *peri*-dichalcogenides were exposed to increasing concentrations of acids, which resulted in extreme broadening, coalescence, and eventually complete disappearance of their ^{1}H and ^{13}C NMR signals, attributed to the formation of paramagnetic species. The original spectra were restored upon addition of excess pyridine-d_5.

During the assays of diselenides **1b**−**1g** for GPx-like activity, where both hydrogen peroxide and benzyl thiol were present, such peak broadening was also observed but was less evident because of the low concentration of the catalyst (10 mol %).[25] Moreover, the presence of trifluoroacetic acid (TFA) resulted in a significantly faster rate of reaction with **1b** than that in its absence (entries 4 and 5 in Table 1). When pyridine-d_5 was included instead of TFA, the reaction rate was considerably suppressed (entry 6, Table 1). These results are parallel to those for the PCET reaction of naphthalene *peri*-diselenides, where TFA promoted NMR peak broadening and coalescence, while pyridine-d_5 reversed the effect. While it is therefore tempting to assume that the formation of the radical and radical cation species from PCET enhances the catalytic activity of **1b** in the presence of TFA, this effect could instead reflect the increased reactivity of hydrogen peroxide through its protonation by the acid or *via* the in situ formation of the corresponding peroxytrifluoroacetic acid. In the absence of TFA, where PCET is precluded, we first considered that peak broadening under the normal assay conditions was the result of single-electron transfer (SET instead of PCET) from diselenides **1** to the more electrophilic selenolseleninates **8** or their precursors **7**. However, when diselenide **1b** was treated with 50 mol % of hydrogen peroxide in order to generate an equimolar mixture of **1b** and **8b**, the ^{1}H NMR spectrum of the resulting solution indicated no peak broadening, thereby ruling out this possibility (Figure 5). This experiment suggests that, in the absence of an acid (and associated PCET), the presence

https://doi.org/10.1021/acsomega.2c02286
ACS Omega 2022, 7, 27312−27323

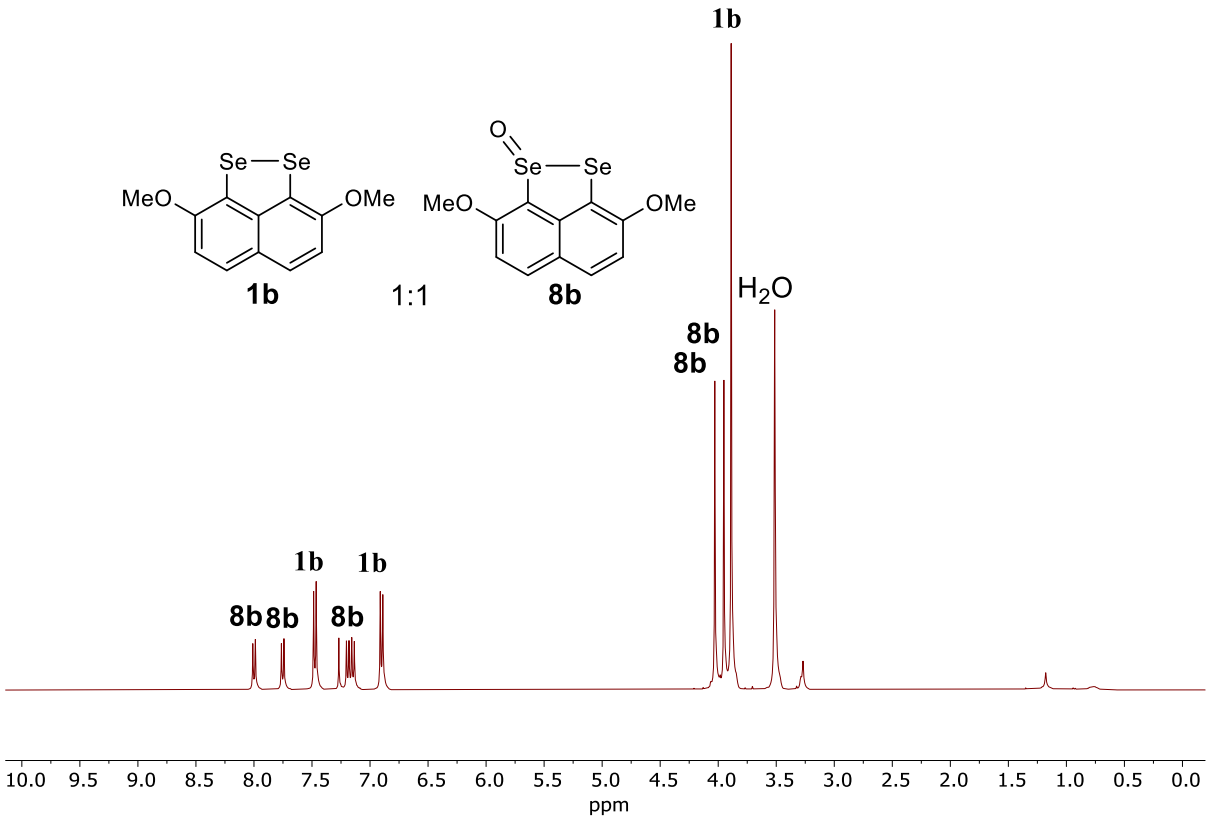

Figure 5. ^{1}H NMR spectrum of 1:1 mixture of diselenide **1b** and selenolseleninate **8b**. The ^{1}H NMR spectrum was obtained in $CDCl_3$-CD_3OD (95:5) at 400 MHz by treating **1b** with 50 mol % of H_2O_2 for 4 h.

of the thiol is required to generate paramagnetic species. We therefore postulate that intermediate **9b**, formed by thiolysis of **8b**[26] (as shown in Scheme 2), serves as the SET acceptor under the conditions of catalytic assay. Further reaction of the selenenyl sulfide moiety of radical **15b** with benzyl thiol then produces radical anion **16b**, followed by charge annihilation and regeneration of **1b**. This tentative mechanism is shown in Scheme 4.[27]

An EPR spectrum of the reaction mixture from **1b** under the usual assay conditions (Figure 6) revealed the presence of paramagnetic species, consistent with the SET process in Scheme 4.[28] An additional experiment was performed to confirm the role of the thiol in initiating radical formation from the otherwise inert 1:1 mixture of diselenide **1b** and selenolseleninate **8b**, as generated in Figure 5. Again, the 1:1 mixture revealed no line broadening in the NMR spectrum (Figure 7a), but when treated with a substoichiometric amount (20 mol %) of benzyl thiol in the absence of hydrogen peroxide, the signals from the diselenide completely disappeared, leaving only those from the remaining unreacted selenolseleninate (Figure 7b). This is consistent with the required formation of **9b** from the reaction of the thiol with **8b** as a precondition to the electron transfer shown in Scheme 4. Finally, the addition of triethylamine to the latter mixture effected an immediate restoration of the NMR signals of diselenide **1b** (Figure 7c). We considered that this could be attributed to the reversal of the formation of **9b** from **8b** under basic conditions, as shown in path A of Scheme 5, or from triethylamine attack at the sulfur atom of **9b** (path B of Scheme 5). However, NMR integration of the methyl signals of **1b** and **8b** at the start and end of the experiment revealed that the proportion of the diselenide relative to the

Scheme 4. SET Reaction of Diselenide 1b after Treatment with Benzyl Thiol

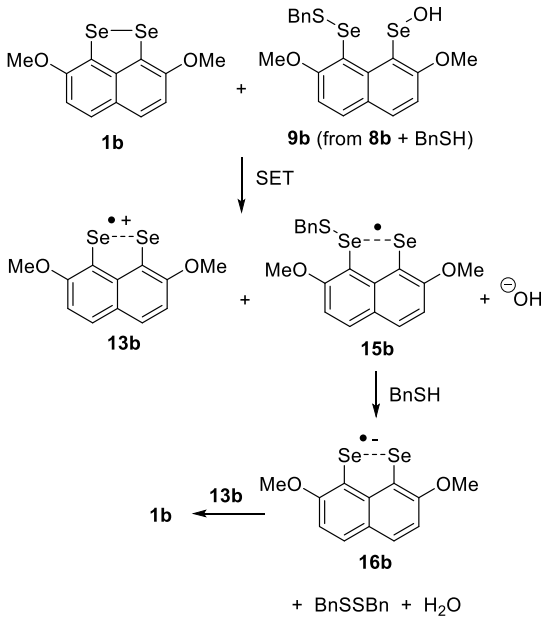

selenolseleninate increased from the initial 1:1 ratio to ca. 1.5:1, as expected from the consumption of 20 mol % of **8b** through its reaction with the thiol to afford an additional 20 mol % of **1b** *via* path B.

A separate experiment related to our previously reported PCET studies was also performed, where **1c** was first treated with 50 mol % of TFA in the absence of hydrogen peroxide

https://doi.org/10.1021/acsomega.2c02286
ACS Omega 2022, 7, 27312−27323

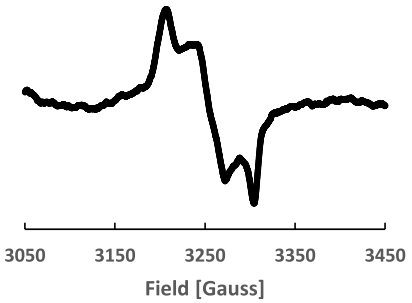

Figure 6. EPR spectrum of diselenide **1b** in the presence of benzyl thiol and hydrogen peroxide under the usual conditions of the antioxidant assay.

Scheme 5. Reaction of Postulated Intermediate 9b with Triethylamine

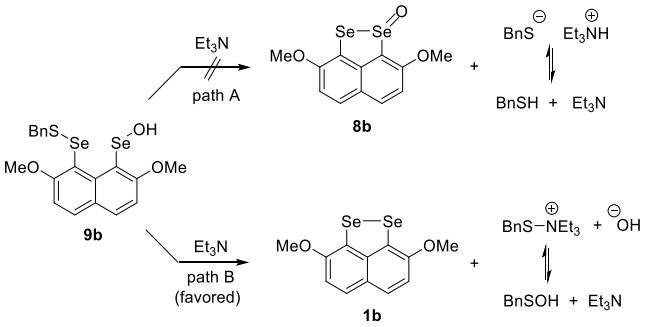

and thiol, resulting in PCET and the usual coalescence and disappearance of ^{1}H NMR peaks. Interestingly, and in contrast to the SET process in the absence of acid, where the presence of thiol is required, the normal NMR spectrum was restored when a large excess of benzyl thiol was added subsequently to that of the acid (Figure 8). While the precise mechanism for

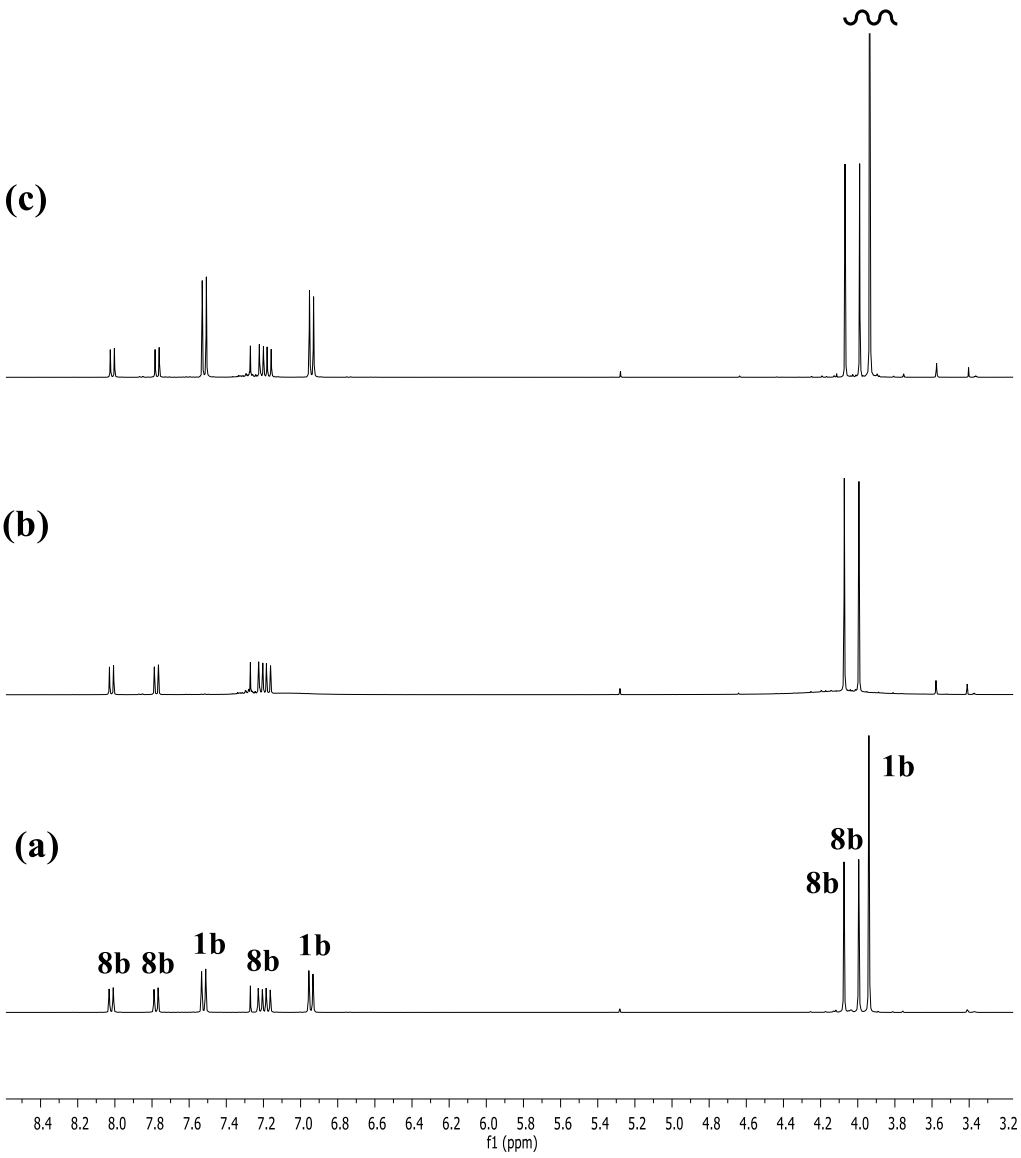

Figure 7. ^{1}H NMR peak broadening during the reaction of diselenide **1b** and selenolseleninate **8b** with benzyl thiol and triethylamine. (a) Spectrum of diselenide **1b** (0.05 mmol) and selenolseleninate **8b** (0.05 mmol); (b) after addition of 0.01 mmol of benzyl thiol; and (c) after addition of 0.036 mmol of triethylamine. ^{1}H NMR spectra were obtained at 400 MHz in $CDCl_3$-CD_3OD (95:5). The complete spectra showing integration and chemical shifts are provided in the Supporting Information.

https://doi.org/10.1021/acsomega.2c02286
ACS Omega 2022, 7, 27312−27323

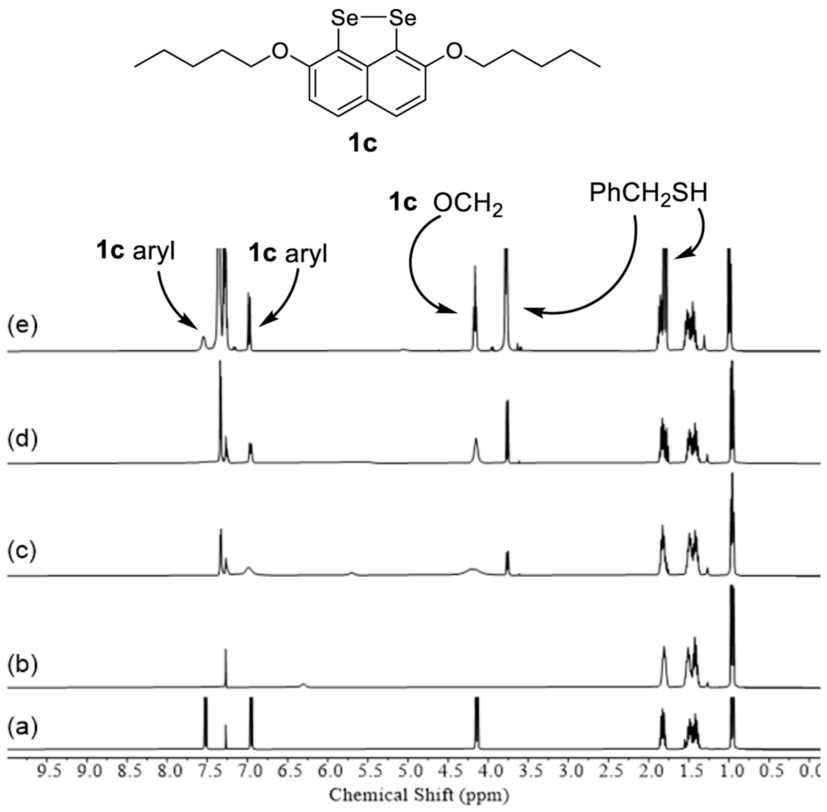

Figure 8. Effect of benzyl thiol and TFA on peak broadening of catalyst **1c**. (a) **1c**: 15.5 mg, 0.034 mmol. (b) TFA: 1.3 μL, 1.9 mg, 0.017 mmol. (c) Benzyl thiol (1st portion): 2.0 μL, 2.1 mg, 0.017 mmol. (d) Benzyl thiol (2nd portion): 2.0 μL, 2.1 mg, 0.017 mmol. (e) Benzyl thiol (3rd portion): 36 μL, 38 mg, 0.306 mmol. The ^{1}H NMR spectra were taken at 400 MHz. The spectra were recorded in 1.0 mL of $CDCl_3$.

this quenching effect is not presently known, it appears that the thiol interrupts the electron transfer step when present in high concentrations.

CONCLUSIONS

In conclusion, the GPx-like catalytic activities of a series of 2,7-dialkoxynaphthalene *peri*-diselenides **1b**−**1g**, including the novel compounds **1e**−**1g**, were measured by means of an NMR-based assay employing hydrogen peroxide as the oxidant and benzyl thiol as the stoichiometric reductant. In particular, the substituents in compounds **1e**−**1g** contain both an oxygen that provides mesomeric electron donation to the diselenide moiety, which is further activated by its constrained conformation, as well as by a second oxygen capable of coordinating with the proximal selenium atom *via* a six- or seven-centered interaction. The anomeric effect in acetals **1e** and **1f** may account for their reduced activities compared to that of the triethylene glycol derivative **1g**, where no such effect is possible. The rate of disulfide formation is also enhanced by TFA and is suppressed by pyridine-d_5.

In the absence of TFA and under the usual assay conditions, peak broadening was again observed and is attributed to a SET reaction where diselenide **1** acts as the electron donor and selenenyl sulfide **9** serves as the acceptor. The possibility that selenolseleninate **8** functions as the electron acceptor instead of **9** was ruled out by the failure to observe NMR peak broadening in an equimolar mixture of **1b** and **8b**, while the dramatic broadening and disappearance of the signals of **1b** upon addition of 20 mol % of benzyl thiol provide further support of **9b** as the acceptor. The regeneration of the diselenide signals at the expense of those of the selenolseleninate when triethylamine was introduced is consistent with interception of **9b** by the amine, resulting in the suppression of SET by removal of the postulated electron acceptor **9b**, while the increase in the ratio of **1b** to **8b** during this process indicates that path B is favored over path A in Scheme 5.

In any event, NMR spectroscopy is highly sensitive to the presence of paramagnetic species and their formation likely comprises a relatively minor side reaction of the processes involved in the assay of GPx-like activity of diselenides **1**. Overall, **1g** affords a ca. three-fold improvement in catalytic activity compared to the previously reported 2,7-dimethoxy derivative **1b**, and the substituents in **1b**−**1g** provide a broad range of hydrophilic and lipophilic properties that may be useful in optimizing the biological activity.

EXPERIMENTAL SECTION

General Experiment. All synthetic reactions were performed using oven-dried glassware under a nitrogen atmosphere, unless otherwise indicated. THF was dried over $LiAlH_4$ and was freshly distilled before use. Hydrogen peroxide was titrated before use and had a concentration of 50 ± 1%. The reported yields are based on isolated products. Reaction temperatures are reported as the temperature of the bath. ^{1}H, ^{13}C, and ^{77}Se NMR spectra were recorded in $CDCl_3$ unless otherwise noted, at 400, 101, and 76 MHz, respectively. Diphenyl diselenide was employed as an external reference (δ 463 ppm relative to Me_2Se) for ^{77}Se NMR spectra.[29] ^{13}C NMR spectra were recorded with broadband proton decoupling. Traces of acid were removed from $CDCl_3$ by treatment with anhydrous K_2CO_3, followed by filtration. NMR multiplets are reported as: s = singlet, d = doublet, t = triplet, q = quartet, and

https://doi.org/10.1021/acsomega.2c02286
ACS Omega 2022, 7, 27312−27323

m = multiplet. HRMS were obtained using either electrospray ionization (ESI) or electron impact (EI), as indicated.2,7-Dihydroxynaphthalene (**3**) was obtained from commercial sources, and compounds **1b**,[17] **1c**,[20] and **6**[30] were prepared, as reported previously.

*2,7-Di(n-dodecyloxy)naphthalene (**4d**).* A mixture of 2,7-dihydroxynaphthalene (**3**) (1.62 g, 10.1 mmol), K_2CO_3 (6.9 g, 50 mmol), and 1-bromododecane (7.5 mL, 7.8 g, 31 mmol) in 30 mL of DMF was heated at 95 °C for 16 h. It was cooled to room temperature and poured into 100 mL of water. The precipitate was filtered, washed with water and methanol, and dried *in vacuo*. The light-brown powder (4.82 g, 96%) was of sufficient purity for use in the next step. A sample was purified by flash chromatography (99:1 hexanes/ethyl acetate) followed by recrystallization from hexanes, to afford 2,7-bis(dodecyloxy)naphthalene as a white solid: mp 60−63 °C; ^{1}H NMR (400 MHz, $CDCl_3$): δ 7.64 (d, J = 8.9 Hz, 2H), 7.04 (d, J = 2.3 Hz, 2H), 6.99 (dd, J = 8.8, 2.4 Hz, 2H), 4.06 (t, J = 6.6 Hz, 4H), 1.85 (crude pentet, J = 7.05 Hz, 4H), 1.56−1.45 (m, 4H), 1.28 (m, 32H), 0.90 (t, J = 6.8 Hz, 6H); ^{13}C{^{1}H} NMR (101 MHz, $CDCl_3$): δ 157.8, 136.2, 129.2, 124.3, 116.4, 106.2, 68.2, 32.1, 29.83, 29.80, 29.78, 29.76, 29.6, 29.51, 29.45, 26.3, 22.9, 14.3; MS (EI-TOF) (m/z, %) 496 (M^+, 100), 328 (5), 160 (10); HRMS (EI-TOF) calcd for $C_{34}H_{56}O_2$ (M^+), 496.4280; found, 496.4280.

*1,8-Dibromo-2,7-di(n-dodecyloxy)naphthalene (**5d**).* *N*-Bromosuccinimide (3.80 g, 21.4 mmol) and pyridine (1.72 mL, 1.68 g, 21.3 mmol) were dissolved in 100 mL of dichloromethane, and 2,7-di(*n*-dodecyloxy)naphthalene (**4d**) (4.82 g, 9.70 mmol) was added. The solution was refluxed for 3 h under a nitrogen atmosphere. The solution was cooled to room temperature and concentrated *in vacuo* to ca. 40 mL. It was then poured into methanol, and the resulting precipitate was filtered, washed with methanol, and dried *in vacuo*. Product **5d** was recrystallized from hexanes as white crystals (4.38 g, 69%): mp 81−82 °C; ^{1}H NMR (400 MHz, $CDCl_3$): δ 7.68 (d, J = 9.0 Hz, 2H), 7.11 (d, J = 8.9 Hz, 2H), 4.14 (t, J = 6.5 Hz, 4H), 1.88 (crude pentet, J = 7.0 Hz, 4H), 1.59−1.50 (m 4H), 1.27 (m, 32H), 0.89 (t, J = 6.8 Hz, 6H); ^{13}C{^{1}H} NMR (101 MHz, $CDCl_3$): δ 156.6, 132.4, 130.3, 127.9, 113.5, 107.3, 70.9, 32.4, 30.14, 30.12, 30.06, 30.04, 29.90, 29.83, 29.81, 26.5, 23.2, 14.6; MS (EI-TOF) (m/z, %) 654 (M^+, 25), 576 (100), 408 (15), 240 (60), 55 (15); HRMS (EI-TOF) calcd for $C_{34}H_{54}{}^{79}Br^{81}BrO_2$ (M^+), 654.2470; found, 654.2461.

*3,8-Di(n-dodecyloxy)naphtho[1,8-cd]-1,2-diselenole (**1d**).* 1,8-Dibromo-2,7-di(*n*-dodecyloxy)naphthalene (**5d**) (1.99 g, 3.04 mmol) was dissolved in 90 mL of dry THF, and the solution was cooled to −78 °C. *n*-Butyllithium (5.13 mL, 1.6 M in hexanes, 8.21 mmol) was then added dropwise, and the reaction mixture was stirred at −78 °C for 30 min, then stirred at 0 °C for 30 min, and for an additional 30 min at room temperature. The solution was then cooled to 0 °C, and elemental selenium (0.676 g, 8.56 mmol) was added. The mixture was warmed to room temperature and stirred for 1 h. The reaction was quenched with saturated NH_4Cl, and air was bubbled through the mixture for 30 min. The mixture was filtered through celite, and the latter was washed with ethyl acetate and dichloromethane. The combined organic layers were washed with brine, dried with anhydrous Na_2SO_4, and evaporated under reduced pressure. The resulting solid was triturated with methanol and diethyl ether until the washings were no longer yellow. Product **1d** was recrystallized from hexanes as purple needles (0.833 g, 42%): mp 84−85 °C; ^{1}H NMR (400 MHz, $CDCl_3$): δ 7.52 (d, J = 8.8 Hz, 2H), 6.95 (d, J = 8.8 Hz, 2H), 4.14 (t, J = 6.4 Hz, 4H), 1.82 (crude pentet, J = 7.0 Hz, 4H), 1.50 (crude pentet, J = 7.3 Hz, 4H), 1.28 (s, 32H), 0.89 (t, J = 6.8 Hz, 6H); ^{13}C{^{1}H} NMR (101 MHz, $CDCl_3$): δ 152.6, 139.9, 127.8, 125.4, 123.6, 113.0, 69.5, 31.9, 29.66, 29.63, 29.58, 29.56, 29.44, 29.35, 26.0, 22.7, 14.1; ^{77}Se{^{1}H} NMR ($CDCl_3$, 76 MHz) δ 405.2; MS (ESI-QTOF) (m/z, %), 655 ([M + H]$^+$, 100), 577 (20), 497 (10), 371 (30), 220 (25), 101 (15); HRMS (EI-TOF) calcd for $C_{34}H_{54}O_2{}^{80}Se_2$ (M^+), 654.2454; found, 654.2475. Anal. Calcd for $C_{34}H_{54}O_2Se_2$: C, 62.56; H, 8.34. Found: C, 62.30; H, 8.09.

*1,8-Dibromo-2,7-di(methoxymethoxy)naphthalene (**5e**).*[31] To a solution of 1,8-dibromonaphthalene-2,7-diol (**6**) (4.74 g, 14.9 mmol) in THF was added NaH (787 mg, 32.8 mmol) at 0 °C, followed by chloromethyl methyl ether (2.48 mL, 2.63 g, 32.7 mmol). The solution was stirred at room temperature for 4 h and then poured into ice-cold water and extracted with ethyl acetate. The organic extracts were combined, washed with water and brine, dried over anhydrous Na_2SO_4, and evaporated *in vacuo*. The crude mixture was purified by flash chromatography (hexanes-ethyl acetate, 2:1, increasing to 3:2) to yield product **5e** as a light brown solid (5.7 g, 94%). This compound decomposed to an intractable black solid after a few days at room temperature. A fresh sample gave: mp 92−94 °C; ^{1}H NMR (400 MHz, DMSO-d_6): δ 7.96 (d, J = 9.0 Hz, 2H), 7.45 (d, J = 9.0 Hz, 2H), 5.41 (s, 4H), 3.45 (s, 6H); ^{13}C{^{1}H} NMR (101 MHz, DMSO-d_6): δ 154.5, 131.2, 130.8, 128.4, 115.6, 106.6, 95.4, 56.6; HRMS (ESI): calcd for $C_{14}H_{14}{}^{79}Br_2O_4$, 404.9332 (M + H); found, 404.9334 (M + H). Anal. Calcd for $C_{14}H_{14}O_4Br_2$: C, 41.41; H, 3.48. Found: C, 41.15; H, 3.48.

*3,8-Di(methoxymethoxy)naphtho[1,8-cd]-1,2-diselenole (**1e**).* *n*-Butyllithium (10.1 mL, 2.5 M in hexanes, 25 mmol) was added to a solution of 1,8-dibromo-2,7-di-(methoxymethoxy)naphthalene (**5e**) (3.7 g, 9.1 mmol) in THF at −78 °C. The solution was slowly warmed to room temperature and then stirred for 1.5 h. It was cooled to 0 °C, elemental selenium (1.98 g, 25.1 mmol) was added, and the solution was stirred for 21 h. It was quenched with aqueous NH_4Cl, and air was bubbled through the solution for 30 min. The solution was extracted with ethyl acetate, and the organic extracts were combined and washed with water and brine, dried over anhydrous Na_2SO_4, and concentrated *in vacuo*. The crude mixture was purified by flash chromatography (dichloromethane/hexanes, 3:1 increasing to 5:1) to yield the product as a purple solid (742 mg, 20%) as well as a second fraction of slightly lower purity (421 mg, 11%). The first fraction gave mp 110−111 °C; ^{1}H NMR (400 MHz, $CDCl_3$): δ 7.51 (d, J = 8.9 Hz, 2H), 7.15 (d, J = 8.9 Hz, 2H), 5.29 (s, 4H), 3.53 (s, 6H); ^{13}C{^{1}H} NMR (101 MHz, CDCl3): δ 150.8, 139.8, 129.1, 125.7, 125.1, 115.2, 95.0, 56.4; ^{77}Se{^{1}H} NMR (76 MHz, $CDCl_3$): δ 408.4. HRMS (EI -TOF): calcd for $C_{14}H_{14}O_4{}^{80}Se_2$, 405.9220; found, 405.9223. Anal. Calcd for $C_{14}H_{14}O_4Se_2$: C, 41.60; H, 3.49. Found: C, 41.76; H, 3.42.

*1,8-Dibromo-2,7-di[(2-methoxyethoxy)methoxy]-naphthalene (**5f**).* The same procedure as in the preparation of **5e** was employed. Product **5f** was obtained from compound **6** (302 mg, 0.950 mmol), sodium hydride (69 mg, 2.9 mmol), and 1-(chloromethoxy)-2-methoxyethane (217 μL, 237 mg, 1.90 mmol). The resulting oil was purified by flash chromatography to afford the product as a red oil (203 mg, 43%). This compound decomposed to an intractable black solid after a few days at room temperature. A fresh sample

https://doi.org/10.1021/acsomega.2c02286
ACS Omega 2022, 7, 27312−27323

gave: ^{1}H NMR (400 MHz, $CDCl_3$): δ 7.72 (d, J = 9.0 Hz, 2H), 7.39 (d, J = 9.0 Hz, 2H), 5.45 (s, 4H), 3.95−3.93 (m, 4H), 3.59−3.57 (m, 4H), 3.37 (s, 6H); ^{13}C{^{1}H} NMR (101 MHz, $CDCl_3$): δ 154.4, 131.6, 129.9, 128.7, 115.4, 107.9, 94.5, 71.5, 68.2, 59.0; HRMS (ESI) calcd for $C_{18}H_{22}{}^{79}Br^{81}BrO_6$, 512.011 (M + NH_4); found, 512.0108 (M + NH_4).

*3,8-Di[2-(methoxyethoxy)methoxy)]naphtho[1,8-cd]-1,2-diselenole (**1f**).* The same procedure as in the preparation of **1e** was employed. Product **1f** was obtained from compound **5f** (1.07 g, 2.17 mmol), *n*-butyllithium (2.4 mL, 2.5 M in hexanes, 6.0 mmol), and elemental selenium (485 mg, 6.14 mmol). The crude product was purified by flash chromatography (hexanes/ethyl acetate, 1:1) to afford a purple oil which solidified upon standing to provide **1f** (447 mg, 42%); mp 64−66 °C; ^{1}H NMR (400 MHz, $CDCl_3$): δ 7.53 (d, J = 8.8 Hz, 2H), 7.21 (d, J = 8.8 Hz, 2H), 5.40 (s, 4H), 3.90−3.87 (m, 4H), 3.58−3.56 (m, 4H), 3.38 (s, 6H); ^{13}C{^{1}H} NMR (101 MHz, $CDCl_3$): δ 150.8, 139.8, 129.1, 125.7, 124.9, 115.2, 94.0, 71.6, 68.0, 59.0; ^{77}Se{^{1}H} NMR (76 MHz, $CDCl_3$): δ 407.9; HRMS (ESI): calcd for $C_{18}H_{22}\ O_6{}^{80}Se_2$, 512.0085 (M + NH_4); found, 512.0068. Anal. Calcd for $C_{18}H_{22}O_6Se_2$: C, 43.92; H, 4.50. Found: C, 43.64; H, 4.37.

*2,7-Di{2-[2-(2-methoxyethoxy)ethoxy]ethoxy}-naphthalene (**4g**).* 2,7-Dihydroxynaphthalene (**3**) (247 mg, 1.54 mmol) and anhydrous K_2CO_3 (1.04 g, 7.54 mmol) were stirred in 30 mL of acetonitrile under nitrogen. 2-[2-(2-methoxyethoxy)ethoxy]ethyl *p*-toluenesulfonate (1.00 g, 3.14 mmol) was then added, and the reaction was refluxed under nitrogen. After 24 h, the opaque, green reaction mixture was cooled to room temperature, washed with saturated $NaHCO_3$, and extracted with ethyl acetate. The combined extracts were dried over anhydrous $MgSO_4$ and concentrated *in vacuo*. The crude product was purified by flash chromatography (ethyl acetate/hexanes, 6:1− to 9:1) to afford 573 mg (82%) of product **4g** as a yellow oil; ^{1}H NMR (400 MHz, $CDCl_3$): δ 7.64 (d, J = 8.7 Hz, 2H), 7.03−7.02 (m, 2H), 7.00 (d, J = 2.4 Hz, 2H), 4.23 (t, J = 4.9 Hz, 4H), 3.92 (t, J = 4.9 Hz, 4H), 3.79−3.74 (m, 4H), 3.72−3.64 (m, 8H), 3.57−3.53 (dd, *m*, 4H), 3.37 (s, 6H); ^{13}C{^{1}H} NMR (101 MHz, $CDCl_3$): δ 157.6, 136.0, 129.3, 124.7, 116.6, 106.6, 72.2, 71.1, 70.9, 70.8, 70.0, 67.7, 59.2; HRMS (ESI-TOF) [M + Na] calcd for $C_{24}H_{36}O_8$, 475.2302; found, 475.2280.

*1,8-Dibromo-2,7-di{2-[2-(2-methoxyethoxy)ethoxy]-ethoxy}naphthalene (**5g**).* Compound **4g** (2.27 g, 5.00 mmol) and pyridine (1.31 mL, 1.28 g, 16.2 mmol) were dissolved in ethyl acetate, followed by NBS (3.74 g, 21.0 mmol), and the solution was stirred at room temperature for 39 h. The mixture was washed with aqueous $NaHCO_3$ and brine, dried over anhydrous Na_2SO_4, and concentrated *in vacuo*. The crude product was purified by flash chromatography (ethyl acetate/methanol, 49:1) to afford 1.10 g (36%) of product **5g** as an orange oil. It was rigorously dried under high vacuum and stored under argon. ^{1}H NMR (400 MHz, $CDCl_3$): δ 7.70 (d, J = 9.0 Hz, 2H), 7.17 (d, J = 9.0 Hz, 2H), 4.31 (t, J = 5.0 Hz, 4H), 3.95 (t, J = 4.9 Hz, 4H), 3.83−3.80 (m, 4H), 3.70−3.61 (m, 8H), 3.55−3.52 (m, 4H), 3.37 (s, 6H); ^{13}C{^{1}H} NMR (100 MHz, $CDCl_3$): δ 156.3, 132.1, 130.1, 128.1, 114.1, 107.7, 72.2, 71.4, 71.0, 70.8, 70.5, 70.0, 59.2; HRMS (ESI-TOF) [M + Na]$^+$ calcd for $C_{24}H_{34}O_8{}^{79}Br_2$, 631.0513; found, 631.0521.

*3,8-Di{2-[2-(2-methoxyethoxy)ethoxy]ethoxy}naphtho-[1,8-cd]-1,2diselenole (**1g**).* The same procedure as in the preparation of **1e** was employed. Product **1g** was obtained from compound **5g** (205 mg, 0.336 mmol), *n*-butyllithium (0.38 mL, 2.5 M, 0.95 mmol), and elemental selenium (122 mg, 1.55 mmol). The crude product was purified by flash chromatography (ethyl acetate) to afford 96 mg (47%) of diselenide **1g** as a purple oil; ^{1}H NMR (400 MHz, $CDCl_3$): δ 7.50 (d, J = 8.9 Hz, 2H), 6.97 (d, J = 8.9 Hz, 2H), 4.29 (crude t, J = 4.5 Hz 4H), 3.87 (crude t, J = 5.0 Hz,, 4H), 3.77−3.75 (m, 4H), 3.70−3.62 (m, 8H), 3.55−3.52 (m, 4H), 3.36 (s, 6H); ^{13}C{^{1}H} NMR (101 MHz, $CDCl_3$): δ 152.5, 140.0, 128.4, 125.7, 124.3, 113.7, 72.1, 71.2, 70.9, 70.7, 70.0, 69.3, 59.2; ^{77}Se{^{1}H} NMR ($CDCl_3$, 76 MHz): δ 408.4; HRMS (ESI-TOF) [M + NH_4]$^+$ calcd for $C_{24}H_{34}O_8{}^{80}Se_2$, 628.0922; found, 629.0900.

General Procedure for the Kinetic Assay of GPx Mimetics. Deuteriochloroform was treated with anhydrous K_2CO_3 to remove acidic impurities before use. DMT (30.1 mg, 0.155 mmol), benzyl thiol (36.3 μL, 38.4 mg, 0.310 mmol), and the catalyst (0.0310 mmol) were dissolved in 10 mL of $CDCl_3$-CD_3OD (95:5). Aqueous hydrogen peroxide (50%, 20.0 μL, 0.350 mmol) was added, and the temperature was maintained at 18 °C with vigorous stirring. The reaction was monitored by ^{1}H NMR spectroscopy, and the amount of dibenzyl disulfide was determined from the integrated ratio of its methylene signal with that of the aromatic signal of DMT. The $t_{1/2}$ for each catalyst was defined as the time required for the formation of 50% of the expected amount of the disulfide.

EPR Spectrum from the Assay of Diselenide 1b. Deuteriochloroform was treated with anhydrous K_2CO_3 to remove acidic impurities before use. DMT (15.0 mg, 0.0772 mmol, internal standard for ^{1}H NMR spectra), benzyl thiol (18.1 μL, 0.154 mmol), and diselenide **1b** (5.3 mg, 0.015 mmol) were dissolved in 5 mL of $CDCl_3$-CD_3OD (95:5). Aqueous hydrogen peroxide (50%, 10.0 μL, 0.18 mmol) was added, and the temperature was maintained at 18 °C. ^{1}H NMR spectra were recorded to ensure that the assay was proceeding in the usual manner with evidence of peak broadening. An aliquot was removed after 2 h, and the EPR spectrum in Figure 6 was obtained at 160 K using an X-band EPR spectrometer operating at 9.6 GHz.[32]

Reaction of Equimolar Amounts of 1b and 8b with Benzyl Thiol and Triethylamine. Diselenide **1b** (35.5 mg, 0.103 mmol) was dissolved in 1 mL of $CDCl_3$-CD_3OD (95:5), and aqueous hydrogen peroxide (50%, 3.1 μL, 0.054 mmol) was added. The reaction was stirred at room temperature for 2 h, at which time a ^{1}H NMR spectrum indicated the presence of equimolar amounts of **1b** and selenolseleninate **8b** (see Figure 7a and Supporting Information 15). Benzyl thiol (1.0 μL, 0.01 mmol) was added, the NMR tube was shaken vigorously, and the NMR spectrum revealed extreme peak broadening of signals from the diselenide (see Figure 7b and Supporting Information 15). While these signals seemed to disappear into the baseline, their presence was detected by integration of the spectrum. Triethylamine (5.0 μL, 0.036 mmol) was then added, the NMR tube was shaken vigorously, and the resulting NMR spectrum showed restoration of the diselenide peaks (see Figure 7c and Supporting Information 16).

PCET Reaction of Diselenide 1c with TFA and Excess Benzyl Thiol. 3,8-Di(*n*-pentyloxy)naphtho[1,8-cd]-1,2-diselenole (**1c**) (15.5 mg, 0.034 mmol) was dissolved in 1.00 mL of $CDCl_3$, and the ^{1}H NMR spectrum was recorded. TFA (1.3 μL, 1.9 mg, 0.017 mmol) was added, and the spectrum was again recorded. Benzyl thiol was added in portions (1st portion: 2.0 μL, 2.1 mg, 0.017 mmol; 2nd portion: 2.0 μL, 2.1 mg, 0.017 mmol; and 3rd portion: 36 μL, 38 mg, 0.306 mmol),

https://doi.org/10.1021/acsomega.2c02286
ACS Omega 2022, 7, 27312−27323

and the spectrum was recorded after each addition (see Figure 8).

■ ASSOCIATED CONTENT

Supporting Information

The Supporting Information is available free of charge at https://pubs.acs.org/doi/10.1021/acsomega.2c02286.

^{1}H, ^{13}C, and ^{77}Se NMR spectra of compounds **1**, **4**, **5**, and **6**, as well as the full spectra from Figure 7 (PDF)

■ AUTHOR INFORMATION

Corresponding Author

Thomas G. Back − *Department of Chemistry, University of Calgary, Calgary, Alberta T2N 1N4, Canada;* orcid.org/0000-0002-3790-1422; Email: tgback@ucalgary.ca

Authors

Adrian I. Doig − *Department of Chemistry, University of Calgary, Calgary, Alberta T2N 1N4, Canada*

Tyler A. Tuck − *Department of Chemistry, University of Calgary, Calgary, Alberta T2N 1N4, Canada*

Brandon LeBlanc − *Department of Chemistry, University of Calgary, Calgary, Alberta T2N 1N4, Canada*

Complete contact information is available at: https://pubs.acs.org/10.1021/acsomega.2c02286

Notes

The authors declare no competing financial interest.

■ ACKNOWLEDGMENTS

We thank the Natural Sciences and Engineering Research Council (NSERC) for financial support (RGPIN-04373). B.L. thanks NSERC for a postgraduate scholarship. We thank Wade White and Michelle Thibeault for assistance with the recording of the EPR spectrum.

■ REFERENCES

(1) Meinwald, J.; Dauplaise, D.; Wudl, F.; Hauser, J. J. *Peri*-bridged Naphthalenes from 1,8-Dilithionaphthalene. *J. Am. Chem. Soc.* **1977**, *99*, 255−257.

(2) (a) Wudl, F. *Organoselenium Chemistry*; Liotta, D., Ed.; John Wiley & Sons: New York, 1987; Chapter 9. (b) Ogura, F.; Takimiya, K. *Organoselenium Chemistry—A Practical Approach*; Back, T. G., Ed.; Oxford University Press: Oxford, U.K., 1999; Chapter 14. (c) Dauplaise, D.; Meinwald, J.; Scott, J. C.; Temkin, H.; Clardy, J. Synthesis and Properties of Chalcogen-Bridged Naphthalenes: A New Series of Electron Donors. *Ann. N.Y. Acad. Sci.* **1978**, *313*, 382−394. (d) Press, D. J.; Back, T. G.; Sutherland, T. C. Charge Transfer Complexes of Electron-Rich Naphthalene Peri-Dichalcogenides with TCNQ. *Tetrahedron Lett.* **2012**, *53*, 1603−1605.

(3) Griffin, J. M.; Knight, F. R.; Hua, G.; Ferrara, J. S.; Hogan, S. W. L.; Woollins, J. D.; Ashbrook, S. E. ^{77}Se Solid-State NMR of Inorganic and Organoselenium Systems: A Combined Experimental and Computational Study. *J. Phys. Chem. C* **2011**, *115*, 10859−10872.

(4) (a) Aucott, S. M.; Milton, H. L.; Robertson, S. D.; Slawin, A. M. Z.; Woollins, J. D. Crystal Structures and Molecular Modeling of 1,8-Chalcogenide-Substituted Naphthalenes. *Heteroat. Chem.* **2004**, *15*, 530−542. (b) Aucott, S. M.; Milton, H. L.; Slawin, A. M. Z.; Woollins, J. D. Crystallographic Studies of Chalcogen Bridged Naphthalenes. *Phosphorus, Sulfur Silicon Relat. Elem.* **2004**, *179*, 985.

(5) For examples, see: (a) Meigh, C. B. E.; Nejman, P. S.; Slawin, A. M. Z.; Derek Woollins, J. Complexation of Aromatic Dichalcogen Ligands to Germanium. *Inorg. Chim. Acta* **2017**, *456*, 120−127. (b) Aucott, S. M.; Milton, H. L.; Robertson, S. D.; Slawin, A. M. Z.; Walker, G. D.; Woollins, J. D. Platinum Complexes of Naphthalene-1,8-dichalcogen and Related Polyaromatic Hydrocarbon Ligands. *Chem.—Eur. J.* **2004**, *10*, 1666−1676.

(6) (a) Manna, D.; Mugesh, G. Regioselective Deiodination of Thyroxine by Iodothyronine Deiodinase Mimics: An Unusual Mechanistic Pathway Involving Cooperative Chalcogen and Halogen Bonding. *J. Am. Chem. Soc.* **2012**, *134*, 4269−4279. (b) Manna, D.; Mugesh, G. Deiodination of Thyroid Hormones by Iodothyronine Deiodinase Mimics: Does an Increase in the Reactivity Alter the Regioselectivity? *J. Am. Chem. Soc.* **2011**, *133*, 9980−9983. (c) Mondal, S.; Mugesh, G. Biomimetic Deiodination of Thyroid Hormones and Iodothyronamines − a Structure-Activity Relationship Study. *Org. Biomol. Chem.* **2016**, *14*, 9490−9500.

(7) (a) Figliola, C.; Male, L.; Horton, P. N.; Pitak, M. B.; Coles, S. J.; Horswell, S. L.; Grainger, R. S. [FeFe]-Hydrogenase Synthetic Mimics Based on Peri-Substituted Dichalcogenides. *Organometallics* **2014**, *33*, 4449−4460. (b) For GPx-like activity of strained fluorene diselenides, see: Jagdev, K.; Tanini, D.; Lownes, J. W.; Figliola, C.; Male, L.; Capperucci, A.; Grainger, R. S. Glutathione Peroxidase Mimics Based on Conformationally-Restricted, *peri*-Like, 4,5-Disubstituted Fluorene Dichalcogenides. *Org. Biomol. Chem.* **2021**, *19*, 10565. Ahead-of-Print article

(8) (a) Sands, K. N.; Tuck, T. A.; Back, T. G. Cyclic Seleninate Esters, Spirodioxyselenuranes and Related Compounds: New Classes of Biological Antioxidants That Emulate Glutathione Peroxidase. *Chem.—Eur. J.* **2018**, *24*, 9714−9728. (b) McNeil, N. M. R.; Press, D. J.; Mayder, D. M.; Garnica, P.; Doyle, L. M.; Back, T. G. Enhanced Glutathione Peroxidase Activity of Water-Soluble and Polyethylene Glycol-Supported Selenides, Related Spirodioxyselenuranes and Pincer Selenuranes. *J. Org. Chem.* **2016**, *81*, 7884−7897. (c) Press, D. J.; McNeil, N. M. R.; Hambrook, M.; Back, T. G. Effects of Methoxy Substituents on the Glutathione Peroxidase-Like Activity of Cyclic Seleninate Esters. *J. Org. Chem.* **2014**, *79*, 9394−9401. (d) Press, D. J.; Mercier, E. A.; Kuzma, D.; Back, T. G. Substituent Effects upon the Catalytic Activity of Aromatic Cyclic Seleninate Esters and Spirodioxyselenuranes That Act as Glutathione Peroxidase Mimetics. *J. Org. Chem.* **2008**, *73*, 4252−4255. (e) Back, T. G.; Kuzma, D.; Parvez, M. Aromatic Derivatives and Tellurium Analogs of Cyclic Seleninate Esters and Spirodioxyselenuranes that Act as Glutathione Peroxidase Mimetics. *J. Org. Chem.* **2005**, *70*, 9230−9236.

(9) For reviews of GPx mimetics, see: (a) Nogueira, C. W.; Rocha, J. B. T. *Organic Selenium and Tellurium Compounds*; Rappoport, Z., Ed.; Wiley: Chichester, U.K., 2012; Vol. 3. Part II; Chapter 21. (b) Wirth, T. Small Organoselenium Compounds: More than just Glutathione Peroxidase Mimics. *Angew. Chem., Int. Ed.* **2015**, *54*, 10074−10076. (c) Bhabak, K. P.; Mugesh, G. Functional Mimics of Glutathione Peroxidase: Bioinspired Synthetic Antioxidants. *Acc. Chem. Res.* **2010**, *43*, 1408−1419. (d) Mugesh, G.; Singh, H. B. Synthetic Organoselenium Compounds as Antioxidants: Glutathione Peroxidase Activity. *Chem. Soc. Rev.* **2000**, *29*, 347−357. (e) Mugesh, G.; du Mont, W.-W.; Sies, H. Chemistry of Biologically Important Synthetic Organoselenium Compounds. *Chem. Rev.* **2001**, *101*, 2125−2180.

(10) (a) Mills, G. C. Glutathione Peroxidase, an Erythrocyte Enzyme Which Protects Hemoglobin from Oxidative Breakdown. *J. Biol. Chem.* **1957**, *229*, 189−197. (b) Rotruck, J. T.; Pope, A. L.; Ganther, H. E.; Swanson, A. B.; Hafeman, D. G.; Hoekstra, W. G. Selenium: Biochemical Role as a Component of Glutathione Peroxidase. *Science* **1973**, *179*, 588−590. (c) Ganther, H. E. Selenoproteins. *Chem. Scr.* **1975**, *8a*, 79−84. (d) Ganther, H. E.; Kraus, R. J. Oxidation States of Glutathione Peroxidase. *Methods Enzymol.* **1984**, *107*, 593−602. (e) Epp, O.; Ladenstein, R.; Wendel, A. The Refined Structure of the Selenoenzyme Glutathione Peroxidase at 0.2-nm Resolution. *Eur. J. Biochem.* **1983**, *133*, 51−69. (f) Flohé, L.; Günzler, W. A.; Schock, H. H. Glutathione Peroxidase: A Selenoenzyme. *FEBS Lett.* **1973**, *32*, 132−134. (g) Flohé, L. Looking Back at the Early Stages of Redox Biology. *Antioxidants* **2020**, *9*, 1254. (h) Brigelius-Flohé, R.; Kipp, A. P.

Physiological Functions of GPx2 and its Role in Inflammation-Triggered Carcinogenesis. *Ann. N.Y. Acad. Sci.* **2012**, *1259*, 19−25.
(11) (a) *Oxidative Stress*; Sies, H., Ed.; Academic Press: London, 1985. (b) *Free Radicals and Oxidative Stress: Environment, Drugs and Food Additives*; Rice-Evans, C., Halliwell, B., Lunt, G. G., Eds.; Portland Press: London, 1995. (c) *Oxidative Processes and Antioxidants*; Paoletti, R., Samuelsson, B., Catapano, A. L., Poli, A., Rinetti, M., Eds.; Raven Press: New York, 1994. (d) *Oxidative Stress and Antioxidants—Their Role in Human Disease*; Rodrigo, R., Ed.; Nova Science Publishers: U.K., 2009. (e) *Role of Oxidative Stress in Chronic Diseases*; Dichi, I., Breganó, J. W., Simão, A. N. C., Cecchini, R., Eds.; CRC Press: Boca Raton, 2014.
(12) (a) Maulik, N.; Yoshida, T.; Das, D. K. Regulation of Cardiomyocyte Apoptosis in Ischemic Reperfused Mouse Heart by Glutathione Peroxidase. *Mol. Cell. Biochem.* **1999**, *196*, 13−21. (b) Dhalla, N.; Elmoselhi, A. B.; Hata, T.; Makino, N. Status of Myocardial Antioxidants in Ischemia-Reperfusion Injury. *Cardiovasc. Res.* **2000**, *47*, 446−456. (c) Mužáková, V.; Kandár, R.; Vojtíšek, P.; Skalický, J.; Vaňková, R.; Čegan, A.; Červinková, Z. Antioxidant Vitamin Levels and Glutathione Peroxidase Activity During Ischemia/Reperfusion in Myocardial Infarction. *Physiol. Res.* **2001**, *50*, 389−396. (d) Crack, P. J.; Taylor, J. M.; de Haan, J. B.; Kola, I.; Hertzog, P.; Iannello, R. C. Glutathione Peroxidase-1 Contributes to the Neuroprotection Seen in the Superoxide Dismutase-1 Transgenic Mouse in Response to Ischemia/Reperfusion Injury. *J. Cereb. Blood Flow Metab.* **2003**, *23*, 19−22. (e) Wong, C. H. Y.; Bozinovski, S.; Hertzog, P. J.; Hickey, M. J.; Crack, P. J. Absence of Glutathione Peroxidase-1 Exacerbates Cerebral Ischemia-Reperfusion Injury by Reducing Post-Ischemic Microvascular Perfusion. *J. Neurochem.* **2008**, *107*, 241−252. (f) Lim, C. C.; Bryan, N. S.; Jain, M.; Garcia-Saura, M. F.; Fernandez, B. O.; Sawyer, D. B.; Handy, D. E.; Loscalzo, J.; Feelisch, M.; Liao, R. Glutathione Peroxidase Deficiency Exacerbates Ischemia-Reperfusion Injury in Male but not Female Myocardium: Insights into Antioxidant Compensatory Mechanisms. *Am. J. Physiol. Heart Circ. Physiol.* **2009**, *297*, H2144−H2153. (g) Landgraf, A. D.; Alsegiani, A. S.; Alaqel, S.; Thanna, S.; Shah, Z. A.; Sucheck, S. J. Neuroprotective and Anti-neuroinflammatory Properties of Ebselen Derivatives and Their Potential to Inhibit Neurodegeneration. *ACS Chem. Neurosci.* **2020**, *11*, 3008−3016. (h) Parnham, M. J.; Sies, H. The early research and development of ebselen. *Biochem. Pharmacol.* **2013**, *86*, 1248−1253.
(13) (a) Dolgin, E. Sound Medicine. *Nat. Med.* **2012**, *18*, 642−644. (b) Kil, J.; Pierce, C.; Tran, H.; Gu, R.; Lynch, E. D. Ebselen Treatment Reduces Noise Induced Hearing Loss via the Mimicry and Induction of Glutathione Peroxidase. *Hear. Res.* **2007**, *226*, 44−51. (c) Lynch, E. D.; Gu, R.; Pierce, C.; Kil, J. Reduction of Acute Cisplatin Ototoxicity and Nephrotoxicity in Rats by Oral Administration of Allopurinol and Ebselen. *Hear. Res.* **2005**, *201*, 81−89. (d) Kil, J.; Lobarinas, E.; Spankovich, C.; Griffiths, S. K.; Antonelli, P. J.; Lynch, E. D.; Le Prell, C. G. Safety and Efficacy of Ebselen for the Prevention of Noise-Induced Hearing Loss: a Randomised, Double-Blind, Placebo-Controlled, Phase 2 Trial. *Lancet* **2017**, *390*, 969−979.
(14) Masaki, C.; Sharpley, A. L.; Godlewska, B. R.; Berrington, A.; Hashimoto, T.; Singh, N.; Vasudevan, S. R.; Emir, U. E.; Churchill, G. C.; Cowen, P. J. Effects of the Potential Lithium-Mimetic, Ebselen, on Brain Neurochemistry: a Magnetic Resonance Spectroscopy Study at 7 Tesla. *Psychopharmacol* **2016**, *233*, 1097−1104.
(15) Marsh, R. E. The Crystal Structure of Diphenyl Diselenide. *Acta Crystallogr.* **1952**, *5*, 458−462.
(16) Back, T. G.; Codding, P. W. Studies of the Dihedral Angle of a Crowded Diselenide by X-ray Crystallography and Ultraviolet Spectroscopy. *Can. J. Chem.* **1983**, *61*, 2749−2752.
(17) Press, D. J.; Back, T. G. Enhanced Glutathione Peroxidase Activity of Conformationally Restricted Naphthalene peri-Dichalcogenides. *Org. Lett.* **2011**, *13*, 4104−4107.
(18) For reviews, see: (a) Mukherjee, A. J.; Zade, S. S.; Singh, H. B.; Sunoj, R. B. Organoselenium Chemistry: Role of Intramolecular Interactions. *Chem. Rev.* **2010**, *110*, 4357−4416. (b) Iwaoka, M.; Arai, K. *Organoselenium Compounds in Biology and Medicine: Synthesis, Biological and Therapeutic Treatments*; Jain, V. K., Priyadarsini, K. I., Eds.; Royal Society of Chemistry: London, U.K., 2018; Chapter 7. For selected examples, see. (c) Iwaoka, M.; Komatsu, H.; Katsuda, T.; Tomoda, S. Nature of Nonbonded Se···O Interactions Characterized by ^{17}O NMR Spectroscopy and NBO and AIM Analyses. *J. Am. Chem. Soc.* **2004**, *126*, 5309−5317. (d) Shimodaira, S.; Asano, Y.; Arai, K.; Iwaoka, M. Selenoglutathione Diselenide: Unique Redox Reactions in the GPx-Like Catalytic Cycle and Repairing of Disulfide Bonds in Scrambled Protein. *Biochemistry* **2017**, *56*, 5644−5653. (e) Zade, S. S.; Panda, S.; Singh, H. B.; Sunoj, R. B.; Butcher, R. J. Intramolecular Interactions Between Chalcogen Atoms: Organoseleniums Derived from 1-Bromo-4-tert-butyl-2,6-di(formyl)benzene. *J. Org. Chem.* **2005**, *70*, 3693−3704. (f) Tripathi, S. K.; Patel, U.; Roy, D.; Sunoj, R. B.; Singh, H. B.; Wolmershäuser, G.; Butcher, R. J. o-Hydroxylmethylphenylchalcogens: Synthesis, Intramolecular Non-bonded Chalcogen···OH Interactions, and Glutathione Peroxidase-like Activity. *J. Org. Chem.* **2005**, *70*, 9237−9247.
(19) The use of coordinating substituents in controlling the outcome of many types of synthetically useful reactions mediated by organoselenium reagents and catalysts has also been reported. For reviews, see: (a) Singh, F. V.; Wirth, T. *The Chemistry of Organic Selenium and Tellurium Compounds*; Rappoport, Z., Ed.; John Wiley and Sons: Chichester, 2012; Vol. 3, Part 1; Chapter 7. (b) Singh, F. V.; Wirth, T. *Organoselenium Chemistry—Synthesis and Reactions*; Wirth, T., Ed.; Wiley-VCH: Weinheim, 2012; Chapter 8.
(20) Tuck, T. A.; Press, D. J.; LeBlanc, B.; Sutherland, T. C.; Back, T. G. Acid-Catalyzed Electron Transfer Processes in Naphthalene peri-Dichalcogenides. *J. Org. Chem.* **2018**, *83*, 11917−11925.
(21) The methyl ester signal of the internal standard was often poorly separated from catalyst peaks, while the aromatic singlet at 8.1 ppm was considerably further downfield from other aromatic signals, providing cleaner integration.
(22) Back, T. G.; Moussa, Z. Diselenides and Allyl Selenides as Glutathione Peroxidase Mimetics. Remarkable Activity of Cyclic Seleninates Produced in Situ by the Oxidation of Allyl ω-Hydroxyalkyl Selenides. *J. Am. Chem. Soc.* **2003**, *125*, 13455−13460.
(23) The poorer reproducibility in the case of **1e** and to a lesser extent **1f**, appears to be due to the gradual formation of an intractable black precipitate, possibly a diselenide polymer, during the assay.
(24) We thank a reviewer for suggesting the possibility that the anomeric effect is the cause of lower reactivity of **1e** and **1f** relative to **1g**.
(25) Close examination of Figure 2 reveals that the aromatic peaks of the naphthalene moiety of **1b** at 6.9 and 7.6 ppm effectively disappear after 3 h.
(26) By analogy, Kice and Liu showed that nucleophiles other than oxyanions react with phenyl benzenethiolsulfinate (PhS(=O)SPh) at the sulfenyl sulfur instead of the sulfinyl sulfur: Kice, J. L.; Liu, C.-C. A. Reactivity of Nucleophiles Toward and the Site of Nucleophilic Attack on Phenyl Benzenethiolsulfinate. *J. Org. Chem.* **1979**, *44*, 1918−1923.
(27) Although benzyl thiol is present as a reactant and the selenenic acids 9 are postulated intermediates in the assay process, the pKa of aliphatic thiols is typically in the range of 10-11 and that for benzeneselenenic acid was estimated to be 11.5. See Kang, S. I.; Kice, J. L. The pKa of Arylselenenic Acids. *J. Org. Chem.* **1986**, *51*, 287−290. Acetic acid (pKa 4.76) only promoted PCET in naphthalene peri-dichalcogenides at high concentrations, as reported in ref. 20. It therefore seems unlikely that benzyl thiol or **9** are sufficiently acidic to effect PCET in the present process.
(28) The EPR spectrum in Figure 6 is similar to the one reported previously under PCET conditions in the presence of TFA (ref 20), suggesting the formation of common radical intermediates, such as radical cation **13b**. However, a sufficiently resolved spectrum could not be obtained to determine the precise structure of the paramagnetic species involved in the process.
(29) Duddeck, H. Selenium-77. Nuclear Magnetic Resonanace Spectroscopy. *Prog. Nucl. Magn. Reson. Spectrosc.* **1995**, *27*, 1−323.

https://doi.org/10.1021/acsomega.2c02286
ACS Omega 2022, 7, 27312−27323

(30) Thirsk, C.; Hawkes, G. E.; Kroemer, R. T.; Liedl, K. R.; Loerting, T.; Nasser, R.; Pritchard, R. G.; Steele, M.; Warren, J. E.; Whiting, A. The Structure, Modelling and Dynamics of 2,7-Diisopropoxy-1,8-diarylnaphthalenes. *J. Chem. Soc., Perkin Trans.* **2002**, *2*, 1510−1519.
(31) Compound **5e** has been reported, but without characterization data. Jia, S.; Li, S.; Liu, Y.; Qin, W.; Yan, H. Enantioselective Control of Both Helical and Axial Stereogenic Elements Through an Organocatalytic Approach. *Angew. Chem., Int. Ed.* **2019**, *58*, 18496−18501.
(32) A control experiment with a mixture of diselenide **1b** and dimethyl terephthalate in the same solvent showed no NMR peak-broadening and an EPR spectrum recorded in the absence of the terephthalate produced the same EPR signal as shown in Figure 6, thus ruling out the formation of radical species by SET from **1b** to the terephthalate.

https://doi.org/10.1021/acsomega.2c02286
ACS Omega 2022, 7, 27312−27323